

# Exploiting the composite character of Rydberg atoms for cold atom trapping

Michael Mayle,<sup>1</sup> Igor Lesanovsky,<sup>2</sup> and Peter Schmelcher<sup>1,3</sup>

<sup>1</sup>*Theoretische Chemie, Universität Heidelberg, D-69120 Heidelberg, Germany*

<sup>2</sup>*Institut für Theoretische Physik, Universität Innsbruck, A-6020 Innsbruck, Austria*

<sup>3</sup>*Physikalisches Institut, Universität Heidelberg, D-69120 Heidelberg, Germany*

(Dated: February 3, 2022)

By investigating the quantum properties of magnetically trapped  $nS_{1/2}$  Rydberg atoms, it is demonstrated that the composite nature of Rydberg atoms significantly alters their trapping properties opposed to point-like particles with the same magnetic moment. We show how the specific signatures of the Rydberg trapping potential can be probed by means of ground state atoms that are off-resonantly coupled to the Rydberg state via a two photon laser transition. In addition, it is demonstrated how this approach provides new possibilities for generating traps for ground state atoms. Simulated time-of-flight pictures mirroring the experimental situation are provided.

PACS numbers: 32.10.Ee, 32.80.Ee, 32.60.+i, 37.10.Gh

The size of Rydberg atoms can easily exceed that of ground state atoms by several orders of magnitude. Already a state with principal quantum number  $n \approx 40$  has an electronic orbit that measures  $\sim 200$  nm in diameter and thus is more than thousand times larger than the ground state [1]. The associated displacement of the atomic charges makes Rydberg atoms highly susceptible to external fields and at the same time is the origin of their strong mutual interaction. The latter has been demonstrated to entail a blockade mechanism [2] thereby effectuating collective Rydberg excitations in ultracold gases [3] and facilitating the observation of conditional dynamics between two single atoms separated by a few  $\mu\text{m}$  [4].

Owed to their large size, Rydberg atoms do not only interact much stronger than their ground state counterparts but also behave quite differently when placed in electric and/or magnetic field configurations that provide trapping for ground state atoms. Several works have focused on this issue, discussing traps for Rydberg atoms based on electric [5], optical [6], or strong magnetic fields [7]. As opposed to ground state atoms, the electronic dynamics usually does not decouple from the external center of mass (c.m.) motion and trapping becomes a particular delicate task. This becomes evident in tight magnetic traps, where the point particle description of the atoms breaks down [8, 9] as the extension of the Rydberg state becomes comparable or even larger than the length scale imposed by the trap, i.e., the extension of the c.m. wave function.

In this letter we illuminate the question of how the composite character of Rydberg atoms, i.e., the fact that it consists of an outer electron far away from a compact ionic core, becomes manifest in standard magnetic traps. In particular, we focus on  $nS_{1/2}$  Rydberg states which are excited from an atomic gas of  $^{87}\text{Rb}$  atoms being in the  $5S_{1/2}, F = m_F = 2$  ground state, as done experimentally in Refs. [3]. We demonstrate that, although both states possess the same magnetic moment, the trapping

potential of the Rydberg states is substantially altered due the composite nature of the atom. This effect can be directly measured by off-resonantly coupling the ground and the Rydberg state via excitation lasers. The subsequent evolution of the dressed ground state atoms is qualitatively modified by the admixture of the Rydberg potential surface leaving its imprint in the time-of-flight (TOF) expansion image. In this context we show that dressing ground state atoms with Rydberg states has the potential to become a useful method to design trapping potentials which are not simply achievable by means of magnetic fields.

As the basic ingredient for magnetically trapping Rydberg atoms, we consider the Ioffe-Pritchard (IP) field configuration given by  $\mathbf{B}(\mathbf{x}) = \mathbf{B}_c + \mathbf{B}_l(\mathbf{x})$  with  $\mathbf{B}_c = B\mathbf{e}_3$ ,  $\mathbf{B}_l(\mathbf{x}) = G[x_1\mathbf{e}_1 - x_2\mathbf{e}_2]$ . The corresponding vector potential reads  $\mathbf{A}(\mathbf{x}) = \mathbf{A}_c(\mathbf{x}) + \mathbf{A}_l(\mathbf{x})$ , with  $\mathbf{A}_c(\mathbf{x}) = \frac{B}{2}[x_1\mathbf{e}_2 - x_2\mathbf{e}_1]$  and  $\mathbf{A}_l(\mathbf{x}) = Gx_1x_2\mathbf{e}_3$ ;  $B$  and  $G$  are the Ioffe field strength and the gradient, respectively. Along the lines of Ref. [8], we model the mutual interaction of the highly excited valence electron and the remaining closed-shell ionic core of a Rydberg atom by an effective potential which depends only on the distance of the two particles. After introducing relative and c.m. coordinates ( $\mathbf{r}$  and  $\mathbf{R}$ ) and employing the unitary transformation  $U = \exp[\frac{i}{2}(\mathbf{B}_c \times \mathbf{r}) \cdot \mathbf{R}]$ , the Hamiltonian describing the Rydberg atom becomes (atomic units are used unless stated otherwise)

$$H = H_A + \frac{\mathbf{P}^2}{2M} + \frac{1}{2}[\mathbf{L}_r + 2\mathbf{S}] \cdot \mathbf{B}_c + \mathbf{S} \cdot \mathbf{B}_l(\mathbf{R} + \mathbf{r}) + \mathbf{A}_l(\mathbf{R} + \mathbf{r}) \cdot \mathbf{p} + \frac{1}{2}\mathbf{A}_c(\mathbf{r})^2 + H_{\text{corr}}. \quad (1)$$

Here,  $H_A = \mathbf{p}^2/2 + V_l(r) + V_{so}(\mathbf{L}_r, \mathbf{S})$  is the field-free Hamiltonian of the valence electron whose core penetration, scattering, and polarization effects are accounted for by the  $l$ -dependent model potential  $V_l(r)$  (see Ref. [10] for its explicit form) while  $\mathbf{L}_r$  and  $\mathbf{S}$  denote its orbital angular momentum and spin, respectively. The spin-orbit interaction is given by  $V_{so}(\mathbf{L}_r, \mathbf{S}) = \frac{\alpha^2}{2}(1 -$

$\frac{\alpha^2}{2} V_l(r) \Big)^{-2} \frac{1}{r} \frac{dV_l(r)}{dr} \mathbf{L}_r \cdot \mathbf{S}$ ; the term  $(1 - \alpha^2 V_l(r)/2)^{-2}$  has been introduced to regularize the nonphysical divergency near the origin [11].  $H_{\text{corr}} = -\boldsymbol{\mu}_c \cdot \mathbf{B}(\mathbf{R}) + \frac{1}{2} \mathbf{A}_l(\mathbf{R} + \mathbf{r})^2 + \frac{1}{M} \mathbf{B}_c \cdot (\mathbf{r} \times \mathbf{P}) + U^\dagger [V_l(r) + V_{so}(\mathbf{L}_r, \mathbf{S})] U$  are small corrections which can be safely neglected in the parameter regime we are focusing on;  $\boldsymbol{\mu}_c$  is the magnetic moment of the nucleus. Note that, in contrast to the low angular momentum states discussed in this letter, mostly circular states are considered in Refs. [8, 9] which allows employing a purely Coulombic potential and neglecting the fine structure. Since the  $Z$ -component of the c.m. momentum commutes with the Hamiltonian (1), the longitudinal motion can be integrated out by employing plane waves. In order to solve the remaining coupled Schrödinger equation, we employ a Born-Oppenheimer separation of the c.m. motion and the electronic degrees of freedom. We are thereby led to an electronic Hamiltonian for fixed c.m. position of the atom whose eigenvalues  $E_\kappa(\mathbf{R})$  depend parametrically on the c.m. coordinates. These adiabatic electronic surfaces serve as potentials for the quantized c.m. motion. The emerging non-adiabatic (off-diagonal) coupling terms between different electronic states can be neglected in our parameter regime [8].

For fixed total electronic angular momentum  $\mathbf{J} = \mathbf{L}_r + \mathbf{S}$ , approximate expressions for the adiabatic electronic energy surfaces can be derived. For this reason, we reformulate the electronic Hamiltonian as [8]

$$H_e = H_A + \frac{1}{2} [\mathbf{L}_r + 2\mathbf{S}] \cdot \mathbf{B}(\mathbf{R}) + GXYp_z + H_r \quad (2)$$

where  $H_r = \mathbf{A}_l(\mathbf{r}) \cdot \mathbf{p} + \mathbf{B}_l(\mathbf{r}) \cdot \mathbf{S} + \frac{1}{2} \mathbf{A}_c(\mathbf{r})^2$  only depends on the relative coordinate. Since in the desired parameter regime  $H_r$  solely represents an energy offset to the electronic energy surfaces, we will omit its contribution in the following. The first two terms of the Hamiltonian (2) can be diagonalized analytically by applying the spatially dependent transformation  $U_r = e^{-i\gamma(L_x + S_x)} e^{-i\beta(L_y + S_y)}$  which rotates the  $z$ -axis into the local magnetic field direction. The corresponding rotation angles are defined by  $\sin \gamma = -GY/\sqrt{B^2 + G^2(X^2 + Y^2)}$  and  $\sin \beta = -GX/\sqrt{B^2 + G^2X^2}$ . The transformed Hamiltonian then becomes

$$U_r H_e U_r^\dagger = H_A + \frac{1}{2} g_j J_z \sqrt{B^2 + G^2(X^2 + Y^2)} + H' \quad (3)$$

with  $g_j = \frac{3}{2} + \frac{s(s+1) - l(l+1)}{2j(j+1)}$  and  $H' = GXYU_r p_z U_r^\dagger$ . Like for ground state atoms, the second term of Eq. (3) represent the coupling of a point-like particle to the magnetic field via its magnetic moment  $\boldsymbol{\mu} = \frac{1}{2} \mathbf{L}_r + \mathbf{S}$ . For a given state  $|\kappa\rangle = |nljm_j\rangle$  with field-free electronic energy  $E_\kappa^{el}$ , this gives rise to the electronic potential energy surface  $E_\kappa^{(0)}(\mathbf{R}) = E_\kappa^{el} + \frac{1}{2} g_j m_j |\mathbf{B}(\mathbf{R})|$ , which is rotationally symmetric around the  $Z$ -axis and confining for  $m_j > 0$ . For small radii ( $\rho = \sqrt{X^2 + Y^2} \ll B/G$ ) an expansion up to second order yields a harmonic potential  $E_\kappa^{(0)}(\rho) \propto \frac{1}{2} M \omega^2 \rho^2$  with a trap frequency of  $\omega =$

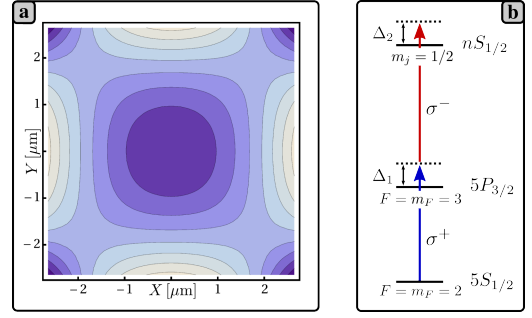


FIG. 1: (a) Contour plot of the  $40S_{1/2}, m_j = 1/2$  Rydberg surface for  $B = 1$  G and  $G = 10$  Tm $^{-1}$ . The loss of the azimuthal symmetry introduced by the composite nature of the Rydberg atom as given by Eq. (4) is evident. The depth of the minimum along the diagonals corresponds to  $\sim 18 \hbar\omega$ ,  $\omega = 2\pi \times 1.3$  kHz being the trap frequency of the harmonic confinement at the origin. (b) Idealized level scheme for an off-resonant two photon coupling of the ground and Rydberg state of  $^{87}\text{Rb}$ . In a IP trap, additional atomic levels and polarizations contribute away from the trap center, see text.

$G\sqrt{g_j m_j / 2MB}$ . At this point, let us briefly comment on the role of the hyperfine interaction. For Rydberg atoms and the regime of field strengths we are considering, the hyperfine interaction can be treated perturbatively while for ground state atoms, on the other hand, one must consider the total angular momentum  $\mathbf{F} = \mathbf{J} + \mathbf{I}$  ( $\mathbf{I}$  being the nuclear spin) yielding energy surfaces  $\sim \frac{1}{2} g_F m_F |\mathbf{B}(\mathbf{R})|$  with  $g_F = g_j \frac{F(F+1) + j(j+1) - I(I+1)}{2F(F+1)}$ . As a consequence, the  $nS_{1/2}, m_j = 1/2$  Rydberg and  $5S_{1/2}$  ground state energy surface are identical for  $F = m_F = 2$ , which we consider in the following.

Within the given approximations, the composite character of the Rydberg atom is manifest in the remaining term  $H'$  of the Hamiltonian (3). It contributes only for large radii close to the diagonal  $X = Y$  and can be treated perturbatively. While it vanishes in first order, second order perturbation theory yields [13]

$$E_\kappa^{(2)}(\mathbf{R}) = G^2 X^2 Y^2 \sum_{\kappa' \neq \kappa} (E_\kappa^{el} - E_{\kappa'}^{el}) \times |\langle \kappa | U_r z U_r^\dagger | \kappa' \rangle|^2 \quad (4)$$

Since  $E_\kappa^{(0)}(\mathbf{R})$  resembles the confinement of ground state atoms, we will attribute  $E_\kappa^{(2)}(\mathbf{R})$  to the composite nature of the Rydberg atom. For  $nS_{1/2}$  Rydberg states, Eq. (4) gives rise to  $E_\kappa^{(2)}(\mathbf{R}) = -C \cdot G^2 X^2 Y^2$  where  $C = 0.48$  for  $n = 40$ . One particular property of the additional contribution  $E_\kappa^{(2)}(\mathbf{R})$  is its spatial dependence: Unlike  $E_\kappa^{(0)}(\mathbf{R})$  it does not preserve the azimuthal symmetry. In Fig. 1(a) this behaviour is illustrated for the example of  $n = 40$ ,  $B = 1$  G,  $G = 10$  Tm $^{-1}$ . Moreover, far from the trap center, but close to the diagonal  $X = Y$ , the character of the potential surface eventually changes from trapping to anti-trapping. Hence, by effectively altering the trap geometry the composite nature distinguishes the Ryd-

berg atom from its point-like counterparts. We remark that the relative difference between the analytical energy surface  $E_{\kappa}^{(0)}(\mathbf{R}) + E_{\kappa}^{(2)}(\mathbf{R})$  and the numerical diagonalization of Hamiltonian (1) is less than 1% for the case of Fig. 1(a); for smaller  $G$  or higher  $B$  the agreement is even better. Hence, the validity of the perturbative approach is ensured for a wide range of field strengths.

Because of the finite lifetime of Rydberg atoms and their strong susceptibility to external perturbations (stray electric fields, mutual interactions etc.), the experimental observation of the composite character might be a difficult task. However, these restrictions can be alleviated by employing the following scheme. Instead of completely transferring a ground state  $^{87}\text{Rb}$  atom to a certain  $nS_{1/2}$  Rydberg state, we rather couple it off-resonantly by a two photon laser transition. This procedure results in a dressed ground state atom whose trapping potential is effectively altered by the admixture of the Rydberg surface. Any change in the ground state c.m. wave function can then be attributed to the composite nature of the Rydberg atom since both possess the same magnetic moment.

Let us investigate the excitation scheme that is frequently encountered in experiments [3]: Laser 1, which is  $\sigma^+$  polarized, drives the transition  $s \rightarrow p$  detuned by  $\Delta_1$  while a second,  $\sigma^-$  polarized laser then couples to the Rydberg state  $n \equiv nS_{1/2}$ ,  $F = m_F = 2$ , with  $s$  denoting the ground state  $5S_{1/2}$ ,  $F = m_F = 2$  and  $p$  the intermediate state  $5P_{3/2}$ ,  $F = m_F = 3$ . The complete two photon transition is supposed to be off-resonant by  $\Delta_2$ , c.f., Fig. 1(b). In the dipole approximation, the interaction of an atom with a laser field is given by  $H_l = \boldsymbol{\epsilon} \cdot \mathbf{r} E_0 \cos \omega t$  with  $\boldsymbol{\epsilon}$  being the polarization vector of the excitation laser. However, since in a IP trap the quantization axis is spatially dependent the polarization vector  $\boldsymbol{\epsilon}$  is only well-defined as  $\sigma^+$  or  $\sigma^-$  at the trap center. In the rotated frame of reference, i.e., after applying the unitary transformation  $U_r H_l U_r^\dagger$ , contributions of all polarizations emerge. Hence, the excitation scheme becomes more involved: Intermediate states with  $F, m_f \in [1, 3]$  contribute as well, while on the Rydberg side also  $m_j = -1/2$  becomes accessible. Altogether, this yields an excitation scheme including 12 atomic levels. In the following, we distinguish two complementary regimes: (a) strong Ioffe fields where simplifications lead to an analytical solution, and (b) high gradients where a numerical treatment is indispensable. In both cases, the time-dependence of the Hamiltonian is removed by employing the rotating wave approximation while the intermediate levels are eliminated by a strong off-resonance condition.

Most insights in the underlying physics can be gained in the regime of strong Ioffe fields  $B$  (and/or weak gradients  $G$ ) where the quantization axis is predominantly defined by the Ioffe field. Selection rules then allow us to revert to the more simple 3-level scheme  $s \leftrightarrow p \leftrightarrow n$

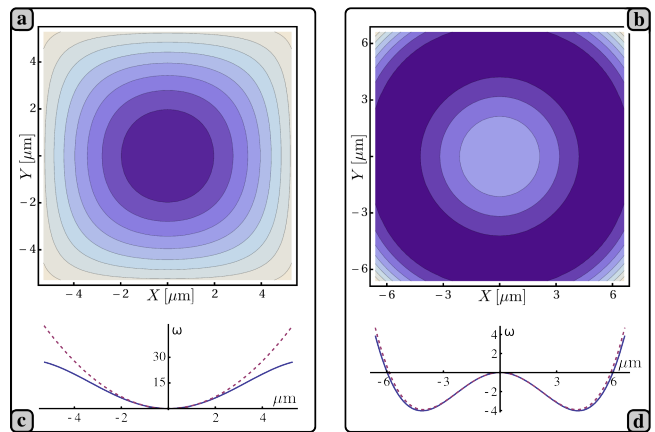


FIG. 2: (a) Contour plot of the dressed ground state surface  $E_-$  for  $n = 40$ ,  $B = 10$  G, and  $G = 5$   $\text{Tm}^{-1}$ . (c) Section along  $X = Y$  of the same energy surface. The deviation from the harmonic confinement of non-dressed ground state atoms (dashed line) due to the composite nature of the Rydberg atom is evident. The energy scale is given in terms of the trap frequency  $\omega = 2\pi \times 200$  Hz. (b) and (d) The same as on the left panel but for  $B = 1$  G,  $G = 5$   $\text{Tm}^{-1}$ . In this high gradient regime the Rabi frequency and therefore the light shift  $V_s$  exhibit a strong spatial dependence resulting in the maximum at the trap center; for the dashed line the contribution  $E_{\kappa}^{(2)}(\mathbf{R})$  of the composite character is omitted. Without dressing, a ground state atom would experience a trap frequency of  $\omega = 2\pi \times 638$  Hz. For values of the Rabi frequencies and detunings see text.

and incorporate the residual, albeit rather weak spatial dependence in the one photon Rabi frequencies

$$\omega_{ps} = \frac{1}{2}(\cos \gamma + \cos \beta - i \sin \gamma \sin \beta) \cdot \omega_{ps}^{(0)} = \omega_{sp}^* \quad (5)$$

$$\omega_{np} = \frac{1}{2}(\cos \gamma + \cos \beta + i \sin \gamma \sin \beta) \cdot \omega_{np}^{(0)} = \omega_{pn}^* \quad (6)$$

$\omega_{ij}^{(0)} = E_{0,ij} \langle i | \boldsymbol{\epsilon}_{ij} \cdot \mathbf{r} | j \rangle$  being the Rabi frequency at the trap center. Employing the rotating wave approximation and adiabatically eliminating the intermediate  $5P_{3/2}$  state eventually provides us a 2-level system

$$\mathcal{H}_{2l} = \begin{pmatrix} \Delta_2 + \tilde{E}_n + V_n & -\Omega/2 \\ -\Omega^*/2 & \tilde{E}_s + V_s \end{pmatrix} \quad (7)$$

with an effective Rabi frequency of

$$\Omega = \frac{\omega_{ps}\omega_{np}}{4} \left[ \frac{1}{\tilde{E}_s - \tilde{E}_p - \Delta_1} + \frac{1}{\tilde{E}_n - \tilde{E}_p + \Delta_2 - \Delta_1} \right] \quad (8)$$

and light shifts of  $V_n = -|\omega_{np}|^2/4(\tilde{E}_p - \tilde{E}_n + \Delta_1 - \Delta_2)$  and  $V_s = -|\omega_{ps}|^2/4(\tilde{E}_p - \tilde{E}_s + \Delta_1)$ . The involved energy surfaces are given by  $\tilde{E}_p = 2|\mathbf{B}(\mathbf{R})|$ ,  $\tilde{E}_s = \frac{1}{2}|\mathbf{B}(\mathbf{R})|$ , and  $\tilde{E}_n = \tilde{E}_s - C \cdot G^2 X^2 Y^2$ , respectively. Neglecting the composite character in the limit  $\Delta_1 \gg \Delta_2$ , one recovers  $\Omega = -\omega_{ps}\omega_{np}/2\Delta_1$ ,  $V_n = -|\omega_{np}|^2/4\Delta_1$ , and  $V_s = -|\omega_{ps}|^2/4\Delta_1$ . The diagonalization of the Hamiltonian (7) yields the dressed Rydberg and ground state

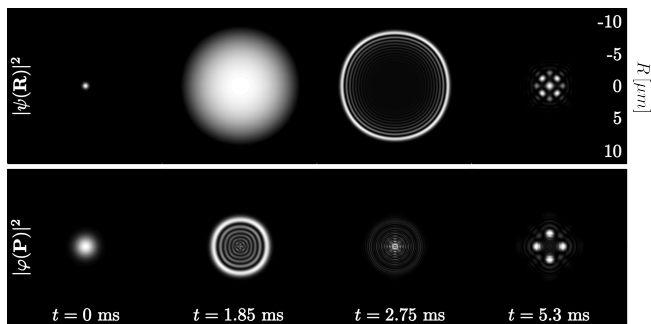


FIG. 3: Temporal evolution of the probability density of a dressed ground state atom in position (upper row) and momentum (lower row) space, respectively. The momentum distribution simulates TOF expansion measurements. Being initially in the lowest non-dressed c.m. eigenstate with a trap frequency of  $\omega = 2\pi \times 638$  Hz, the atom subsequently evolves in the potential given in Fig. 2(b). The time scale of 5 ms corresponds to the first oscillation of the c.m. wave packet. The loss of the azimuthal symmetry due to the composite character of Rydberg atoms is evident once the wave function has probed the outer parts of the potential surface ( $t > 2.75$  ms).

surfaces  $E_{\pm}$ . For large detunings  $\Delta_2 \gg \Omega$  one can approximate

$$E_- \approx \tilde{E}_s + V_s - \frac{\Omega^2}{4\Delta_2} + \frac{\Omega^2}{4\Delta_2^2}(\tilde{E}_n + V_n - \tilde{E}_s - V_s), \quad (9)$$

i.e., the contribution of the Rydberg surface to the dressed ground state trapping potential is suppressed by the factor  $(\Omega/\Delta_2)^2$ . Furthermore, any spatial variation in the light shift  $V_s$  and in the Rabi frequency  $\Omega$  will effectively alter the trapping potential experienced by the dressed ground state atom. As an example, let us investigate the configuration  $B = 10$  G,  $G = 5$  Tm $^{-1}$ ,  $\omega_{ps}^{(0)} = \omega_{np}^{(0)} = 2\pi \times 30$  MHz,  $\Delta_1 = -2\pi \times 220$  MHz, and  $\Delta_2 = -2\pi \times 10$  MHz. In this case, the contribution Eq. (4), which derives from the composite nature of the Rydberg atom, prevents the Rydberg potential from supporting any confined c.m. state. This strong deviation from the point-like behaviour is consequently mirrored in the dressed ground state potential: Along  $X = Y$ , where the effect of Eq. (4) is most pronounced, the trapping potential is gradually lowered compared to the harmonic confinement of the non-dressed ground state, c.f., Fig. 2(c). As a consequence, the two-dimensional trapping potential loses its azimuthal symmetry, see Fig. 2(a).

Another situation arises for strong gradients where the approximation of a 3-level system breaks down and the full 12-level system must be solved for accurate results. In Figure 2(b) and (d) the results of such a calculation are shown for the specific example of  $B = 1$  G,  $G = 5$  Tm $^{-1}$ ,  $\omega_{ps}^{(0)} = 2\pi \times 75$  MHz,  $\omega_{np}^{(0)} = 2\pi \times 30$  MHz,  $\Delta_1 = -2\pi \times 430$  MHz, and  $\Delta_2 = -2\pi \times 50$  MHz. For this configuration, the light shift  $V_s$  develops a strong

spatial dependence which results in a qualitative change of the dressed ground state potential, namely, from a parabolic to a ring-shaped behaviour. A wave packet initially prepared in the non-dressed c.m. ground state disperses in such a potential while being reflected at the outer repulsive walls, leading to breathing oscillations. In this way, the outer parts of the dressed potential surface, where the composite character of the Rydberg atom becomes manifest, are probed. Simulated TOF expansion images reveal the influence of the Rydberg admixture, c.f., Fig. 3: The observed four-fold symmetry after one oscillation ( $t = 5.3$  ms) is solely due to the contribution  $E_{\kappa}^{(2)}(\mathbf{R})$ ; its absence would conserve the azimuthal symmetry, i.e., the ring shaped pattern.

Let us finally comment on the experimental feasibility. The proposed dressed states possess a finite effective lifetime which can be estimated by  $\tau = \tau_n/|c|^2$  with  $|c|^2 = (\Omega/2\Delta_2)^2$  being the two-level admixture coefficient of the Rydberg state and  $\tau_n$  its radiative lifetime. With  $\tau_{40} \approx 70$   $\mu$ s [12], the strong gradient configuration yields  $\tau \approx 87$  ms which is more than one order of magnitude longer as the timescale of the envisaged dynamics. Similarly, the van der Waals interaction of two Rydberg atoms is suppressed by  $|c|^4$ . Since the latter interaction is not accounted for in our calculations, the resulting energy shift  $\delta$  on the Rydberg levels should be marginal, i.e., well below the excitation detuning  $\Delta_2$ . Taking  $\delta < 2\pi \times 1.0$  MHz as an example (compared to  $|\Delta_2| = 2\pi \times 50$  MHz) yields a minimum interparticle distance of  $\sim 250$  nm, which is feasible even for condensate densities.

To conclude, we demonstrated that the composite nature of Rydberg atoms is crucial for their trapping properties. Our approach allows to measure the specific features of the  $nS_{1/2}$  Rydberg trapping potential by means of ground state atoms that are off-resonantly coupled to the Rydberg level. Moreover, the proposed approach facilitates the designing of trapping potentials for ground state atoms, which is demonstrated by means of the example of a ring-shaped trap.

This work was supported by the German Research Foundation (DFG) within the framework of the Excellence Initiative through the Heidelberg Graduate School of Fundamental Physics. P.S. acknowledges financial support by the DFG, M.M. from the Landesgraduiertenförderung Baden-Württemberg.

- 
- [1] T. F. Gallagher, *Rydberg Atoms* (Cambridge University Press, Cambridge, England, 1994).
  - [2] D. Tong *et al.*, Phys. Rev. Lett. **93**, 063001 (2004); T. Vogt *et al.*, *ibid.* **99**, 073002 (2007); K. Singer *et al.*, *ibid.* **93**, 163001 (2004); T. Cubel Liebisch *et al.*, *ibid.* **95**, 253002 (2005); **98**, 109903(E) (2007).
  - [3] R. Heidemann *et al.*, Phys. Rev. Lett. **99**, 163601 (2007); M. Reetz-Lamour *et al.*, *ibid.* **100**, 253001 (2008).

- [4] E. Urban *et al.*, Nat. Phys. **5**, 110 (2009); A. Gaëtan *et al.*, *ibid.* **5**, 115 (2009).
- [5] P. Hyafil *et al.*, Phys. Rev. Lett. **93**, 103001 (2004).
- [6] S. K. Dutta *et al.*, Phys. Rev. Lett. **85**, 5551 (2000).
- [7] J.-H. Choi *et al.*, Phys. Rev. Lett. **95**, 243001 (2005).
- [8] B. Hezel, I. Lesanovsky, and P. Schmelcher, Phys. Rev. Lett. **97**, 223001 (2006); Phys. Rev. A **76**, 053417 (2007).
- [9] M. Mayle *et al.*, Phys. Rev. Lett. **99**, 113004 (2007).
- [10] M. Marinescu, H. R. Sadeghpour, and A. Dalgarno, Phys. Rev. A **49**, 982 (1994).
- [11] E. U. Condon and G. H. Shortley, *The Theory of Atomic Spectra* (Cambridge University Press, Cambridge, England, 1935).
- [12] A. L. de Oliveira *et al.*, Phys. Rev. A **65**, 031401(R) (2002).
- [13] We approximated  $p_z = i[H_A, z] - i[V_i(r) + V_{so}, z] \approx i[H_A, z]$  since the second term is energetically suppressed in perturbation theory.